IEEE Access
Multidisciplinary | Rapid Review | Open Access Journal

Received July 31, 2019, accepted September 3, 2019, date of publication September 13, 2019, date of current version September 26, 2019.

Digital Object Identifier 10.1109/ACCESS.2019.2941009

A Sequential MCMC Model for Reliability Evaluation of Offshore Wind Farms Considering Severe Weather Conditions

HUAWEI CHAO[1,2], BO HU[1], (Member, IEEE), KAIGUI XIE[1], (Senior Member, IEEE), HENG-MING TAI[3], (Senior Member, IEEE), JIAHAO YAN[1], (Student Member, IEEE), AND YANLIN LI[1], (Student Member, IEEE)

[1]State Key Laboratory of Power Transmission Equipment and System Security at Chongqing University, Chongqing 400044, China
[2]State Grid Sichuan Economic Research Institute, Sichuan, Chengdu 60000, China
[3]Department of Electrical and Computer Engineering, University of Tulsa, Tulsa, OK 74104, USA

Corresponding author: Bo Hu (hboy8361@163.com)

This work was supported in part by the National Natural Science Foundation of China under Project 51677011, and in part by the National Science Fund for Distinguished Young Scholars of China under Project 51725701.

ABSTRACT The offshore wind farms (OWF) are susceptible to the severe weather, which can cause the increase of component failure rate and has significant influence on the maintenance process and the reliability of wind farms. This paper proposes a sequential Markov chain Monte Carlo (MCMC) model for reliability evaluation of the OWF considering the impact of severe offshore weather. First, main factors affecting the wind turbine (WT) failure rate are analyzed. Second, a time-varying analytical model for the WT failure rate affected by wind speed and lightning is established. Three types of WT failure rates are considered: the failure rate under normal weather, that under strong wind, and that affected by lightning. Moreover, a time-varying analytical model for the repair time of main components of OWF is established by considering the influence of severe weather on offshore transportation time and maintenance efficiency after component failure. The MCMC model takes into account the temporal correlation of the weather and the repair process of failed component in the reliability evaluation. The model enables simultaneous simulation of the weather intensity and component state. For each system state generated by the MCMC model, a breadth-first search (BFS) method is applied to analyze the connectivity of the WTs and the sink node. Finally, the output of the wind farm is determined based on the wind speed data at this state. The expected energy not supply (EENS) and the generation ratio availability (GRA) indices of the OWF are evaluated to demonstrate the effectiveness of the proposed models. Further, the effects of other factors such as the enhanced protection for WT, the use of helicopter, and the weather characteristics of the OWF location on the reliability of OWF are discussed.

INDEX TERMS Offshore wind farm, reliability evaluation, severe weather, failure rate, repair time, Markov chain Monte Carlo.

I. INTRODUCTION

Countries around the world have put considerable effort to increase the use of renewable energy. The wind power has been one of the focused energy sources because of its rich reserves, pollution-free characteristic and low development cost. According to the European Wind Energy Association (EWEA), due to the strong development of onshore wind power and offshore wind power, the planned installed capacity of European wind power will reach 392 GW by 2030 [1].

The associate editor coordinating the review of this manuscript and approving it for publication was Baoping Cai.

Since the offshore wind farms (OWFs) have the advantages of less land occupancy, higher average wind speed, and more sufficient annual utilization hours compared with the onshore wind farms, the development of large-scale OWF has attracted considerable attention [2]. However, OWFs require high maintenance costs and long repair time. This underlines the importance of reliability evaluation in the planning stage of OWF.

Many studies on the reliability evaluation of onshore wind farms have been reported, but relatively few are on OWFs. Two types of wind farm reliability evaluation modeling methods are available, the chronological simulation

method [3], [4] and the analytical method [5]–[7]. The former considers the time correlation of WT output, and enables simple calculation of the actual frequency index. The computation and storage demands, however, are high for its time-consuming simulation [8]. On the other hand, even though the analytical method is relatively simple to perform the system state enumeration process, it encounters the ''curse of dimensionality'' problem when the system size is large [9].

The operating environment of OWFs is more complex than that of the onshore wind farms because it is located at sea. The effect of offshore severe weather condition must be considered in the evaluation of the reliability of OWF [10], [11]. The impact is mainly reflected on the equipment failure rate and repair time parameters during reliability evaluation [10]. Most OWFs in use were built in recent years, as compared with the onshore wind power industry [12]. The reliability parameters of offshore WT and the collection system components are insufficient. Thus, most existing OWF reliability evaluations use the statistical data from the onshore wind farm [11]. The conclusion of the above analysis found that the key to accurately assessing the reliability of OWF is to modify the reliability parameters to reflect the impact of severe offshore weather [13].

Several studies on the impact of severe offshore weather on the reliability parameters of OWF components are available [14]–[16]. The reliability of OWF considering seasonal weather changes was analyzed and the effect on the failure rate and repair time parameters of the main components of OWF was presented [14]. The reliability parameters of the OWF components in the normal weather and the severe weather were evaluated according to the engineering experience [15]. In [16], the availability of OWF considering the inaccessibility problem caused by excessive wind and wave was investigated. The above studies consider the impact of severe weather on component reliability parameters in the reliability evaluation of OWF mainly on the qualitative analysis of historical operational experience, not much on the quantitative influence of the weather intensity on component reliability. Moreover, the temporal correlation between the component reliability parameter and the weather intensity in the reliability evaluation is missing. The variations of weather intensity are not factored into the component reliability parameters.

This paper proposes a Markov chain Monte Carlo (MCMC) model that can simulate both the weather intensity and the component state. The proposed model takes into account the temporal correlation of the weather and the repair process of component outage in the reliability evaluation. As a result, the adverse effect due to severe weather conditions on the OWF output can be quantified. The MCMC model facilitates the reliability evaluation by considering the failure rate of the offshore WT under three conditions: the failure rate at the normal weather, the failure rate affected by wind speed, and the failure rate affected by lightning (according to historical data). A time-varying repair time model for the main components of OWF is also constructed by considering the influence of the severe weather on maintenance efficiency after component failure. For each system state generated by the MCMC model, the connectivity between the WT and the sink node is checked based on the BFS algorithm, and the output of the wind farm is determined by the wind speed sample. The correctness and effectiveness of the proposed model and method are verified on an OWF in China. It can provide an accurate estimation of OWF output and guidance for system operator from the reliability perspective.

The rest of the paper is organized as follows. Section II discusses the influence of severe weather on reliability parameters of OWF and determine the main weather factors that affect the OWF reliability. Section III presents the time-varying failure rate and repair time model of OWF components. The reliability evaluation method of OWF is proposed in Sections IV. Case studies are carried out in Section V. Section VI concludes this paper.

II. INFLUENCE OF SEVERE WEATHER ON RELIABILITY PARAMETERS OF OWF

The impact of severe weather on the reliability of OWF components is mainly reflected in two aspects: The increased component failure rate and the prolonged repair time after failure. The weather at OWF is severe if any weather intensity exceeds a specified threshold, and the corresponding threshold will be analyzed later. The following provides brief analysis.

(1) Main components of OWF include the WTs, submarine cables, transformers, and breakers. Due to the height of WT and its wind driven characteristic, the impact of severe weather on the reliability of WT is obvious and significant [17]. It has been reported [18], [19] that the WT failures are mainly originated from mechanical components such as gearboxes and blades, and more than 70% of blade failures are caused by lightning strikes or strong winds. Other components such as cables, circuit breakers, etc. are relatively less affected by weather conditions due to their location on the seabed or inside the cabinet. Hence, this paper mainly considers the effects of severe weather on the failure rate of WT. In particular, the proposed model investigates the impact of strong winds and lightning. The detailed modeling approach is presented in Section 3.1.

(2) When the failure occurred in severe weather conditions such as strong winds or large waves, maintenance crew and spare parts cannot reach the wind farm immediately for maintenance due to weather constraints [16]. Moreover, lightning also affects the maintenance process. So this paper mainly accounts for the impact of strong winds, large waves and lightning strikes when considering the repair time of OWF components. The detailed calculation method for the repair time of OWF components under severe weather will be introduced in Section 3.2.

III. TIME-VARYING FAILURE RATE AND REPAIR TIME MODEL OF OWF COMPONENTS

This study characterizes the WT failure rate and the repair time of all components as time-varying functions varying with the weather intensity to describe the impact of severe weather on failure rate and repair time of the OWF components. It describes the relationship between the component failure and repair process to the weather intensity during the same time period.

A. TIME-VARYING FAILURE RATE MODEL

Assume that the failure rate of the WT in the time period t (taken as 1 hour) does not change. Inspired by the modeling method of the overhead transmission lines failure rate in severe weather [20], the time-varying failure rate of the offshore WT can be expressed as

$$\lambda(t) = \lambda_{\text{normal}} + \lambda_{\text{wind}}(t) + \lambda_{\text{lightning}}(t). \tag{1}$$

In (1), $\lambda(t)$ is the WT failure rate in the period t, λ_{normal} is the average failure rate of the WT in the period t under normal weather, $\lambda_{\text{wind}}(t)$ is the correction to failure rate due to strong winds and $\lambda_{\text{lighting}}(t)$ is that due to lightning. λ_{normal} can be obtained from the historical WT failure statistics under normal conditions. $\lambda_{\text{wind}}(t)$ is a function of the average wind speed $v(t)$ and $\lambda_{\text{lighting}}(t)$ is a function of the ground flash density $N_{\text{g}}(t)$.

1) TIME-VARYING FAILURE RATE MODEL OF WT AFFECTED BY THE WIND SPEED

The relationship between the wind speed and WT failure probability is given in [33]

$$U(t) = \begin{cases} U_0, & v(t) \le v_r \\ \dfrac{1}{1+(\frac{1}{U_0}-1)e^{-b(v(t)-v_r)}}, & v(t) > v_r, \end{cases} \tag{2}$$

where $U(t)$ is the unavailability of the WT in the period t and U_0 is the WT unavailability under normal wind speed condition ($v(t) \le v_r$). v_r is the rated wind speed of the WT and b is a parameter greater than zero, which represents the fragility of the WT under the strong wind condition. Larger b implies strong influence on the failure rate by the wind speed variation. In this study, the value of b is set as 0.15 [21].

Assume that the repair rate μ of the WT is constant. Then the unavailability of the WT can be expressed as [22]

$$U(t) = \frac{\lambda(t)}{\lambda(t)+\mu}. \tag{3}$$

In normal weather, the WT unavailability U_0 can be expressed as

$$U_0 = \frac{\lambda_{\text{normal}}}{\lambda_{\text{normal}}+\mu}. \tag{4}$$

Substituting (3) and (4) into (2) and some algebra manipulation yields the relationship between the failure rate of the WT and the wind speed during the period t:

$$\lambda(t) = \begin{cases} \lambda_{\text{normal}}, & v(t) \le v_r \\ (\dfrac{1}{e^{-b(v(t)-v_r)}})\lambda_{\text{normal}}, & v(t) > v_r. \end{cases} \tag{5}$$

Subtracting the average hourly failure rate of the WT in normal weather from (5), the correction of the WT failure rate affected by strong winds during the period t can be obtained

$$\lambda_{\text{wind}}(t) = \begin{cases} 0, & v(t) \le v_r \\ (\dfrac{1}{e^{-b(v(t)-v_r)}}1)\lambda_{\text{normal}}, & v(t) > v_r. \end{cases} \tag{6}$$

2) TIME-VARYING FAILURE RATE MODEL OF WTS AFFECTED BY LIGHTNING

Through statistical analysis of historical WT lightning failure records in [23], [24], it can be found that the frequency of the serious lightning strike failure of the WT and the lightning strike frequency suffered by the WT are approximately linearly related

$$\lambda_{\text{lightning}}(t) = kN_L(t). \tag{7}$$

In (7), k is a scalar parameter greater than zero and N_L is the number of lightning strikes to WT. Based on the data from [24] for $\lambda_{\text{lightning}}$ and N_L, it is found that k is 0.2186.

The frequency of lightning strikes on tall structures exposed to air can be modeled as a function of the height of the object and the external lightning density [25]. It can be applied to analyze the relationship between the expected number of the lightning strikes on WT and the ground flash density during period t

$$N_L(t) = 24 \times 10^{-6} h_s^{2.05} N_g(t), \tag{8}$$

where h_s is the height of the WT and $N_{\text{g}}(t)$ is the ground flash density of the period t.

Substituting (8) into (7), we obtain the relationship between the corrected failure rate and the lightning intensity

$$\lambda_{\text{lightning}}(t) = k \times 24 \times 10^{-6} h_s^{2.05} N_g(t). \tag{9}$$

B. TIME-VARYING REPAIR TIME MODEL FOR OWF

The maintenance crew and spare parts may not be able to reach the damaged area on time after the failure of OWF components due to the poor transportation conditions. This often results in the prolonged maintenance time. Even in normal weather, the maintenance efficiency varies in different weather conditions and different seasons. These factors also cause the changes in the component repair time.

To accommodate such uncertainties, the repair time of OWF components comes from two sources. One is the waiting and transportation time WT(t) of the maintenance crew and component spare parts. Another is the on-site maintenance time $R_e(t)$. Then the component repair time $r(t)$ at period t can be expressed as

$$r(t) = WT(t) + R_e(t). \tag{10}$$

Fig. 1 depicts the configuration of the component repair time. Details are given below.

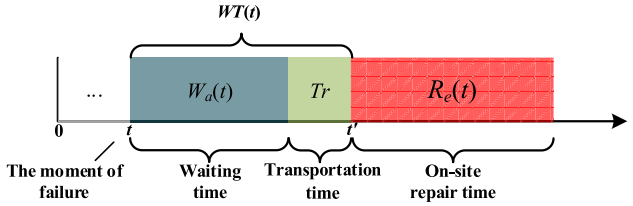

FIGURE 1. Composition of repair time $r(t)$.

1) WAITING AND TRANSPORTATION TIME OF MAINTENANCE RESOURCES $WT(t)$

According to [26], when the wind speed $v(t) \leq 15$ m/s and the significant wave height $h(t) \leq 2$m, The maintenance crew and spare parts can be safely transported to the failed site. That is, the weather is not severe and the maintenance resources are accessible to OWF. In addition, according to engineering experience, if lightning strike occurs ($N_g(t) > 0$), the offshore maintenance is deemed unsuitable and the OWF is unable to tap into the maintenance resources.

The transportation time of the maintenance resource is Tr and the on-site repair time is $R_e(t)$. The waiting time needed to meet the transportation and maintenance requirements must be counted. These requirements specify that the wind speed has to be less than 15m/s, the height of significant wave less than 2m, and the ground flash density is 0. The length of the time interval is at least $Tr + R_{ep}(t)$, where R_{ep} is the estimated on-site repair time. The waiting time to meet the transportation and maintenance requirements is represented by $W_a(t)$ and can be obtained from the weather intensity data. The waiting and transportation time $WT(t)$ of the maintenance resource can be expressed as:

$$WT(t) = W_a(t) + Tr \tag{11}$$

2) REPAIR TIME $R_E(t)$ CONSIDERING MAINTENANCE EFFICIENCY

The repair time varies along with the maintenance efficiency. The efficiency of maintenance crew differs in different seasons, due to the climatic factors. In addition, weather factors such as wind speed also affect the efficiency of maintenance crew. The following examines the influence of seasonal factors and wind speed on the maintenance efficiency and maintenance time.

In the four seasons of spring, summer, autumn and winter, the working efficiency of maintenance crew in OWF is different. Generally, the maintenance efficiency in spring and autumn is higher than that in winter and summer. So the repair time of the same type of failure in spring and autumn is shorter than that in winter and summer. This paper defines the seasonal weight factor ks to account for the seasonal effect. The weight factor can be obtained from historical maintenance records. Table 1 shows the seasonal weight factors used in this study [27].

The wind speed also affects the maintenance efficiency. When the wind speed exceeds the critical value v_{crit}, the maintenance efficiency will be affected [28]. The higher

TABLE 1. The weight factor of different seasons.

Season	k_s
Spring	1.00
Summer	1.35
Autumn	1.00
Winter	1.50

the wind speed, the lower the maintenance efficiency and the longer the maintenance time. Since the transportation of maintenance resources, as well as on-site maintenance, are always carried out at a significant wave height of less than 2m and a ground flash density of 0, this paper does not consider the impact of waves and lightning on the maintenance efficiency.

Based on the above analysis, the repair time $R_e(t)$ considering the maintenance efficiency can be expressed as

$$R_e(t) = \begin{cases} k_s(t')r_{\text{normal}}, & v(t') \leq v_{crit} \\ [1 + \omega \times (v(t') - v_{crit})]k_s(t')r_{\text{normal}}, & v_{crit} < v(t') \leq 15. \end{cases} \tag{12}$$

r_{normal} is the average repair time (excluding the waiting and transportation time) of the failed component under normal weather conditions, which have the significant wave height less than 2m, ground flash density $= 0$, wind speed lower than v_{crit}, and season is spring or autumn. t' is the start time of actual repair. $k_s(t')$ is the seasonal weight factor. $v(t')$ is the average wind speed for the period of $[t', t' + r_{\text{normal}}]$. Parameter $\omega > 0$ is used to describe the influence of wind speed on the maintenance time. The larger the ω is, the higher the influence of wind speed on the maintenance time. v_{crit} is the wind speed threshold. The value of v_{crit} and ω are $v_{crit} = 8$ m/s, $\omega = 0.4$ [28].

IV. RELIABILITY EVALUATION OF OWF BASED ON THE MCMC METHOD

A Markov chain Monte Carlo (MCMC) based simulation model for offshore weather and component state of OWF is described. The model is used to generate the time series of weather intensity and the component state. Then we investigate the impact of component failure in the OWF and determine the wind farm output of each sample system state. A brief description of the procedures is shown in Fig. 2.

A. MCMC SIMULATION FOR WEATHER INTENSITY AND COMPONENT STATE OF OWF

The offshore weather and the component state are not independent. It has been shown in Section 3 that the component state and the weather intensity during the current and previous time periods are temporally correlated. Simulation is performed to characterize this correlation. The MCMC method is used to generate the time series of weather intensity and state of OWF components for the reliability evaluation of OWF.

MCMC is a method that applies the Markov chain to Monte Carlo simulation. The Gibbs sampler is typically used to generate the Markov chains required in the MCMC method [29].

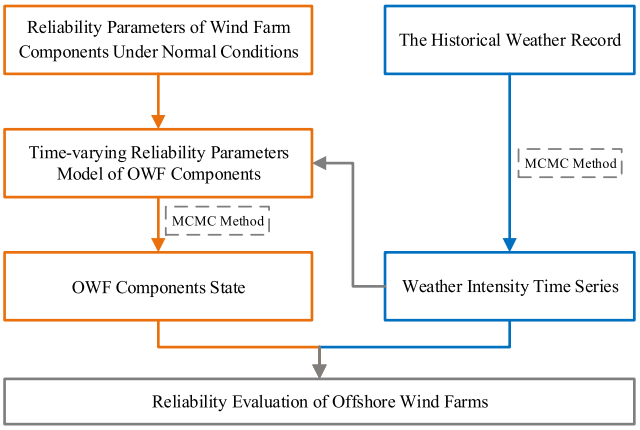

FIGURE 2. The flow chart of proposed model.

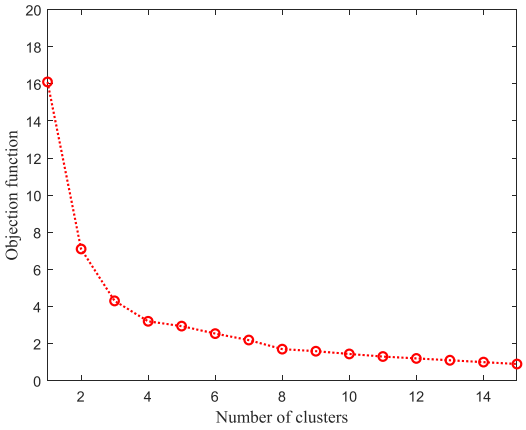

FIGURE 3. The relationship between the number of clusters and the objective function value of the clustering method.

Some definitions regarding the MCMC based simulation method is given below.

(1) Let the wind speed, the significant wave height, and the ground flash density be represented, respectively, by the time series vectors $\mathbf{v}_h = [v_1, v_2, \ldots, v_N]$, $\mathbf{h}_h = [h_1, h_2, \ldots, h_N]$, and $\mathbf{N}_g = [N_{g1}, N_{g2}, \ldots, N_{gN}]$. N is the length of historical data. These three weather data at time t is collected as a column vector $\mathbf{w}_t = [v_t, h_t, N_{gt}]^T$. Then the historical weather record can be expressed as

$$\mathbf{W} = [\mathbf{w}_1, \mathbf{w}_2, \ldots, \mathbf{w}_N] = \begin{bmatrix} v_1 & v_2 & \cdots & v_N \\ h_1 & h_2 & \cdots & h_N \\ N_{g1} & N_{g2} & \cdots & N_{gN} \end{bmatrix}. \quad (13)$$

(2) Suppose that the OWF has a total of M components. Each component has two states: the normal state and the failure state. The failure of the component is independent of each other. Let $x_m^{(t)}$ be the sampled state of the m^{th} component in the period t. If the component m is in the normal state, let $x_m^{(t)} = 0$; if the component m is in the failure state, let $x_m^{(t)} = 1$. The vector $\mathbf{X}^{(t)} = [x_1^{(t)}, \ldots, x_M^{(t)}]$represents the sample state of the entire OWF system in the period t.

(3) Samples of the weather intensity and the OWF components state over the T time periods are stored in $\mathbf{W}'$ and $\mathbf{X}$, respectively.

The following describes the simulation procedure for the offshore weather intensity and OWF components state based on the MCMC method. In this study, the failure rate and the repair time of OWF components are assumed to remain unchanged during period t,

1) Classify the typical offshore weather conditions.
Based on the K-means clustering method [30], the historical offshore weather record $\mathbf{W}= [\mathbf{w}_1, \mathbf{w}_2 \ldots \mathbf{w}_N]$ can be divided into K clusters. Each cluster Ω_i, $i = 1, 2, \ldots, K$, corresponds to a unique weather state S_i, $i = 1, 2, \ldots, K$. The objective function value of the clustering method is reduced by increasing the number of clusters K [31]. When the number of clusters is larger than 6, the objective function value as shown in Fig. 3. Here K takes 8.

2) Calculate the cumulative transition probability matrix between weather conditions.
Let p_{ij} be the state transition probability from the weather state S_i to the weather state S_j. Find the maximum likelihood estimate by

$$p_{ij} = \frac{T_{ij}}{\sum_{k=1}^{N} T_{ik}}. \quad (14)$$

T_{ij} is the total number of the observed transitions from weather state S_i to weather state S_j. The transition probability matrix between K weather states can be expressed as

$$\mathbf{P_w} = \begin{bmatrix} p_{11} & p_{12} & \cdots & p_{1K} \\ p_{21} & p_{22} & \cdots & p_{2K} \\ \vdots & \vdots & \ddots & \vdots \\ p_{K1} & p_{K2} & \cdots & p_{KK} \end{bmatrix}. \quad (15)$$

Then generate the cumulative probability matrix $\mathbf{P}'_w$ of the matrix $\mathbf{P}_w$, and the j^{th} element of the i^{th} row is calculated by

$$p'_{ij} = \begin{cases} 0, & j = 1 \\ \sum_{l=1}^{j-1} p_{il}, & 1 < j \le K+1. \end{cases} \quad (16)$$

Due to the seasonality of weather intensity, this paper calculates the cumulative probability matrix $\mathbf{P}'_w$ of different seasons to accurately describe the transition rate between K weather states. In other words, four $\mathbf{P}'_w$ are generated as $\mathbf{P}'_{SP-w}$, $\mathbf{P}'_{SU-w}$, $\mathbf{P}'_{FA-w}$ and $\mathbf{P}'_{WI-w}$ corresponding to the respective season. *SP*, *SU*, *FA* and *WI* are abbreviations for spring, autumn, summer, and winter, respectively. The matrix $\mathbf{P}'_{SP-w}$ is taken as an example.

3) Let $t = 0$, randomly select the initial weather state S_i of the $t = 0$ period.

4) Simulate the weather state during the period $t+1$ based on the MCMC method.

Let the weather state of the period t be S_i, and generate a random number q_1, which follows a uniform distribution in the interval [0, 1]. If $p'_{ij} < q_1 \leq p'_{i(j+1)}$, the weather state of the period $t+1$ is considered to be S_j [32].

5) Sample the wind speed, the significant wave height, and the ground flash density during the period $t+1$.
The empirical distribution function $F(.)$ of weather intensity is employed to capture the probability distribution characteristics within each weather state. This would provide the support for the accuracy of simulation results. The weather intensity for a specific weather state S_j can be sampled by the following procedure. Take the wind speed as an example. Generate a random number q_2 from a uniform distribution in the [0, 1] interval and calculate

$$F(v(t+1)) = F(v_j^{\min}) + q_2 \times (F(v_j^{\max}) - F(v_j^{\min})), \tag{17}$$

where $v_j^{\min}$ and $v_j^{\max}$ are the minimum and maximum wind speeds that may occur under the weather state S_j, respectively. The interval $[v_j^{\min}, v_j^{\min}]$ is divided into N_e subintervals. Then sample of the wind speed in the period $t+1$ can be obtained by

$$v(t+1) = v_e + \frac{F(v(t+1)) - F(v_e)}{F(v_{e+1}) - F(v_e)}(v_{e+1} - v_e). \tag{18}$$

v_e and v_{e+1} are the upper and lower bounds of the corresponding subinterval within the weather state S_j that satisfies $F(v_e) < F(v(t+1)) \leq F(v_{e+1})$.
The sampled values of the significant wave height and the ground flash density during the period $t+1$ can be obtained by a calculation process similar to the wind speed and will not be described here.

6) Let $t = t+1$, if $t < T$, return to step 4; otherwise, the weather intensity time series of T time periods is obtained. Store it in matrix $\mathbf{W}'$ and proceed to the next step.
7) Let $t = 0$ and all components be in the normal state, that is, $\mathbf{X}^{(0)}$ is a zero vector of $M \times 1$.
8) Calculate the time-varying failure rate $\lambda(t)$ of the offshore WT considering the influence of severe weather based on formula (1), and calculate the time-varying repair time $r(t)$ of the OWF component considering the impact of severe weather based on formula (10). The transition probability matrix of the component state for the Gibbs sampler is expressed as

$$\mathbf{P}_{\mathrm{X}} = \begin{bmatrix} 1-\lambda(t) & \lambda(t) \\ \mu(t) & 1-\mu(t) \end{bmatrix} \tag{19}$$

where $.\mu(t)$ is the component repair rate, which is the reciprocal of the repair time $r(t)$.
9) Determine the component state vector $\mathbf{X}^{(t+1)} = [x_1^{(t+1)}, \ldots, x_{\mathrm{M}}^{(t+1)}]^T$ in the period $t+1$.
Take a component m as an example to describe how to determine the component state in the period $t+1$.

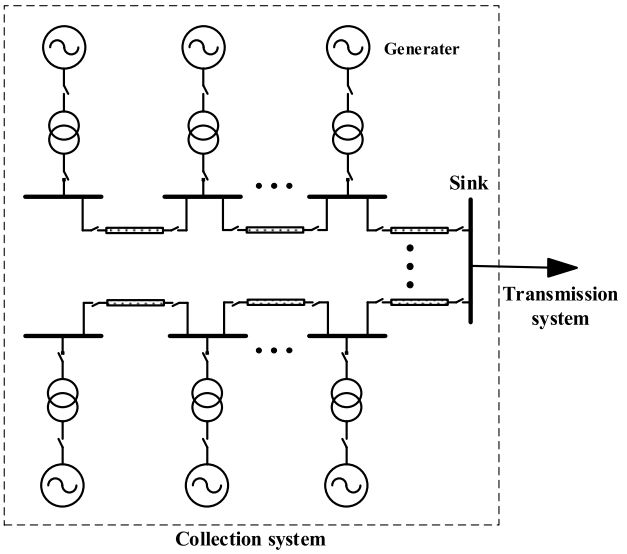

FIGURE 4. Electrical network configuration of an OWF.

Generate a random number q_3 uniformly distributed in the interval [0, 1] and make the judgment according to the following two conditions:
1) Suppose that the component m in the period t is in the normal state. If q_3 is less than 1-.$\lambda(t)$, then the component m stays in the normal state at the period $t+1$. Otherwise, the component is moved to the failure state.
2) Suppose that the component m in the period t is in the failure state. If q_3 is less than 1-.$\mu(t)$, the component m is still in the failure state at the period $t+1$; otherwise, the component is moved to the normal state.
3) Let $t = t+1$, if $t < T$, return to step 8; otherwise, stop and output $\mathbf{W}'$ and $\mathbf{X}$.

B. CALCULATION OF WIND FARM OUTPUT OF THE SAMPLED STATE

A typical OWF system is shown in Fig. 4. It consists of the collection system and the transmission system. This study does not consider the failure impact of the transmission system when assessing the reliability of OWF. The focus is on the impact of the failure of WT and the collection system. Two types of the collection system are available: the string type and the ring type [33]. The configuration in Fig. 4 is the string type.

It can be seen from Fig. 4 that if a single WT or the component connected to WT fail, the WT will be disconnected from system during the failure period and the output is zero. If the cables between the WTs fail, it mainly affects the connectivity between the WT and the Sink node. The affected WTs will be off-grid and their output is zero.

Consider a four-WT OWF system shown in Fig. 5(a). Fig. 5(b) is a connectivity graph representation of Fig. 5(a). In Fig. 5(b), the numbers 1-4 denote four WTs. Each WT includes a low voltage (LV) contactor, tower cable, transformer, and a medium voltage (MV) breaker.

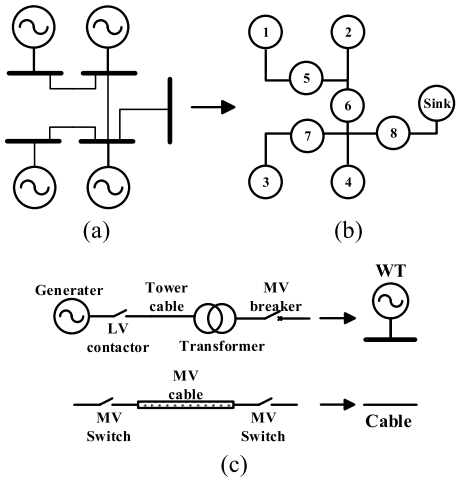

FIGURE 5. Schematic of a simple OWF. (a) Four WTs. (b) Graph representation. (c) Detailed elements of WT and connection cable.

The numbers 5-8 correspond to the connection cable between the WTs. The cable includes the MV Switch directly connected to the cable and cable itself. A brief description to determine the output of a wind farm in a single MCMC state is given below.

1) The output power of the WT in the period t is determined by

$$P_{out}(t) = \begin{cases} 0, & v(t) \le v_{ci} \text{ or } v(t) \ge v_{co} \\ P_r \dfrac{v(t) - v_{ci}}{v_r - v_{ci}}, & v_{ci} \le v(t) \le v_r \\ P_r, & v_r \le v \le v_{co}. \end{cases} \quad (20)$$

In (20), $P_{out}(t)$ is the output power (MW) of the WT at time t, v_{ci} is the cut-in wind speed (m/s), v_r is the rated wind speed (m/s), v_{co} is the cut-off wind speed (m/s), and P_r is the rated output (MW) of the WT.

2) Based on Fig. 5(b), an adjacency matrix [34] $\mathbf{A_1}$ for the components numbered from 1 to 8 is generated.

$$\mathbf{A}_1 = \begin{bmatrix} 1&0&0&0&1&0&0&0 \\ 0&1&0&0&1&1&0&0 \\ 0&0&1&0&0&0&1&0 \\ 0&0&0&1&0&1&1&1 \\ 1&1&0&0&1&1&0&0 \\ 0&1&0&1&1&1&1&1 \\ 0&0&1&1&0&1&1&1 \\ 0&0&0&1&0&1&1&1 \end{bmatrix} \quad (21)$$

$\mathbf{A_1}$ is an 8×8 matrix. The t-time state of the components 1-8 is analyzed according to the vector $\mathbf{X}^{(t)} = [x_1^{(t)}, \ldots, x_M^{(t)}]^T$. If all components are in the normal states, the connectivity graph is formed starting from the Sink node based on the breadth-first search (BFS) algorithm [34] and the adjacency matrix $\mathbf{A_1}$. Since no components fail, WT1 to WT4 are in the connectivity graph and all WTs output normally. The output of the wind farm is the sum of all four WT's output. If WT3 and cable5 fail, the elements in the third and fifth rows and columns of the $\mathbf{A_M}$ matrix are set to zero. The adjacency matrix $\mathbf{A_2}$ in this state is formed and a connectivity graph is generated.

$$\mathbf{A}_2 = \begin{bmatrix} 1&0&0&0&0&0&0&0 \\ 0&1&0&0&0&1&0&0 \\ 0&0&0&0&0&0&0&0 \\ 0&0&0&1&0&1&1&1 \\ 0&0&0&0&0&0&0&0 \\ 0&1&0&1&0&1&1&1 \\ 0&0&0&1&0&1&1&1 \\ 0&0&0&1&0&1&1&1 \end{bmatrix} \quad (22)$$

The connectivity graph is formed based on the BFS algorithm and the adjacency matrix $\mathbf{A_2}$. In the connectivity graph, only the WT2 and WT4 are connected to the Sink node. At this time, the wind farm output is the sum of the output of the WT2 and WT4. Other situations can also be analyzed using the above method.

C. OWF RELIABILITY EVALUATION

The OWF reliability evaluation algorithm considering the impact of severe weather on the component failure and repair process is described below.

1) Sample the Markov chain of the weather intensity and component state of T time length by the proposed MCMC simulation method in Section 4.1.
2) Analyze the system topology in the $\mathbf{X}(t)$ state and calculate the output of the wind farm and the input wind power based on the method in Section 4.2 to obtain the ratio between the output and the input wind power of the wind farm, the power generation rate $GR(t)$. Calculate the difference between the output and the rated maximum output of OWF during the period t to obtain the energy not supply $ENS(t)$ of OWF.
3) Calculate OWF reliability indices Expected Energy Not Supply ($EENS$) and Generation Ratio Availability (GRA) [35]:

$$EENS = \sum_{t=1}^{T} ENS(t) \times 8760/T \quad (23)$$

$$GRA = T_{grc}/T, \quad (24)$$

where T_{grc} is the sum of time when $GR(t) > GRc$ in the T period, and GRc is the criterion generation rate.

V. CASE STUDIES

In this paper, an OWF in China described in [36] is used as an example to validate the proposed MCMC reliability evaluation method under severe weather conditions. Fig. 6 depicts the configuration of the OWF, which consists of 50 WTs rated at 2MW each and with a height of 90m. Cut-in, rated, and cut-out wind speeds of the WT are 4, 12, and 25 m/s, respectively. The hourly wind speed and significant wave height data are from the NOAA website [37]. Ground flash density data are from [28]. The reliability parameters of wind farm components under normal conditions are shown in Table 2.

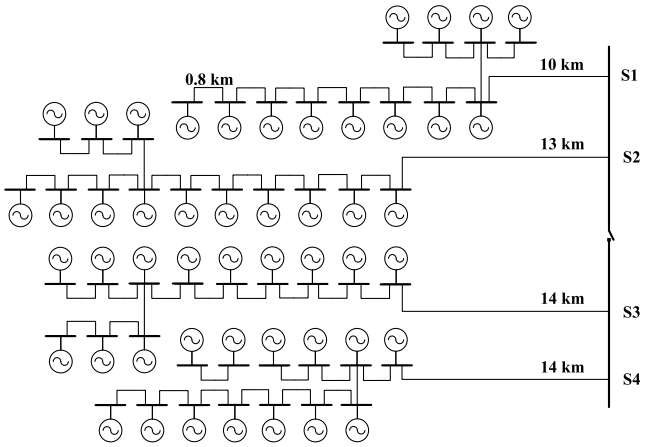

FIGURE 6. Topology of an OWF in China [34].

TABLE 2. Uncorrected component reliability parameters.

Equipment	Failure rate λ (occ./y)	Repair time r_{normal} (h/occ.)
WT	1.5	490
MV switch	0.025	240
MV breaker	0.025	72
LV contactor	0.0667	240
Nacelle transformer	0.0131	240
70 m tower cable	0.015/km	240
MV cable	0.015/km	1440

The transportation time of the maintenance resource is set as 1 hour.

A. RELIABILITY EVALUATION RESULT

The impact of severe weather conditions on the reliability of OWF is evaluated in the following five cases.

Case 1: Not consider the effects of severe weather on component failure rate and repair time.

Case 2: Consider only the effect of strong winds on failure rate.

Case 3: Consider only the effect of lightning strikes on failure rate.

Case 4: Consider only the effect of severe weather on the repair time.

Case 5: Consider the effects of severe weather on the component failure rate and the repair time.

The *GRc* is set as 80%. The Gibbs sampler performs 500,000 samples, and the sampling results are used to evaluate the reliability of OWF. The *EENS* and *GRA* indices of different cases are shown in Table 3. It can be seen from Table 3 that Case 1 has the smallest *EENS* and the largest *GRA*. Thus, not considering the severe weather, the system reliability level is the highest and the utilization of offshore wind power is the most efficient. When the severe weather conditions are factored in, the *EENS* rises and *GRA* falls. This shows that the weather factor cannot be ignored in the reliability evaluation of OWF.

TABLE 3. Reliability indices of different cases.

Case	*EENS* (MWh/y)	*GRA*
Case 1	538134.95	0.8931
Case 2	542744.56	0.8657
Case 3	542518.65	0.8785
Case 4	562205.95	0.7149
Case 5	571492.38	0.6750

Compared to Case 1, *EENS* in Case 2 is increased by 0.9% and *GRA* is decreased by 3.1%. For Case 3, *EENS* is increased by 0.8% and *GRA* is decreased by 1.6%. It can be found that *EENS* index changes slightly when effect of severe weather on component failure rate is considered. This is not the case for the *GRA* index, which increases in a noticeable manner. The *GRA* index emphasizes the energy loss caused by the equipment failure. So the failure of component has more influence on *GRA* than the wind speed variation. The severe weather has considerable impact on the repair time of WT, as evidenced from the results of Case 4 and Case 5. In Case 4, *EENS* increases by 4.5% and *GRA* decreases by 20.0%. When taking both the failure rate and the repair time into account, the *EENS* and *GRA* indices vary even more, *EENS* by 6.2% and *GRA* by 24.4%. This indicates that the impact of severe weather on the reliability of wind farms is mainly reflected on the repair process of the failed component.

B. ENHANCED PROTECTION FOR WT ON OWF RELIABILITY

In order to reduce the impact of strong winds and lightning strikes on the reliability of WT and OWF, the WT can be reinforced. For example, the use of double-layer material blades and regular maintenance of the mechanical structure of the WT are two main measures to improve the wind resistance of the WT [38]. Lightning resistance of the WT can be improved by applying the conducting materials to the blade surface and placing the down conductors inside the blade [39].

It is difficult to accurately quantify the effects of the above measures on wind and lightning resistance of the WT. Here we analyze the impact of the enhanced protection for WT on the reliability by changing the values of relevant parameters. Two actions: One is to characterize the wind resistance of WT under strong winds by changing the value of parameter b in equation (6). The smaller the value of b is, the stronger the WT is. Another is to characterize the lightning resistance of WT by changing the value of parameter k in equation (9). Smaller k implies stronger lightning resistance of WT.

Fig. 7 shows the variation curves of *EENS* and *GRA* of Case 5 when the parameters b and k are respectively changed to 0.95, 0.9, 0.85, 0.8, 0.75, 0.7, 0.65, and 0.6 times of the original value. In Fig. 7, the blue and green curves are for the *EENS* and *GRA* indices under different b and k, respectively. It can be seen from Fig. 7 that as b and k decrease, *EENS* decreases and *GRA* increases, and the OWF reliability is improved.

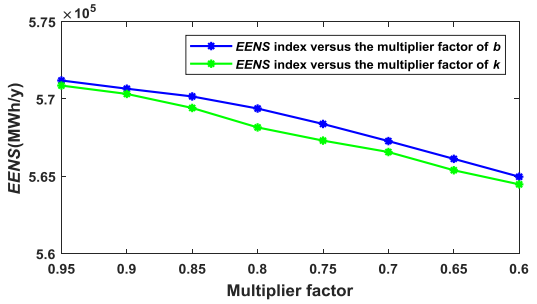

(a)

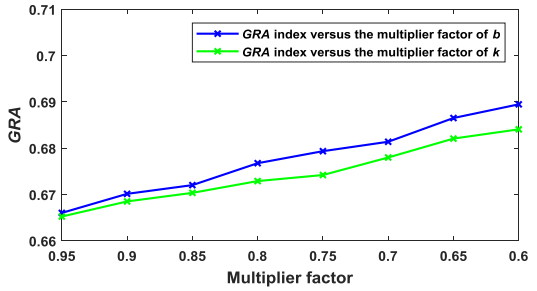

(b)

FIGURE 7. Performance of the reliability indices versus different parameters. (a) *EENS*. (b) *GRA*.

C. IMPACT OF USING HELICOPTER ON THE RELIABILITY OF OWF

Analysis in Section 5.1 shows that the impact of severe weather on the reliability of OWF is mainly reflected on the repair time of the failed component. In order to improve maintenance efficiency, helicopters are used in certain situations to transport the maintenance crew and spare parts. However, the cost by the helicopter is very high compared to that by the ship. It falls into the cost-benefit analysis problem to make a trade-off between the OWF reliability and maintenance cost. This section focuses on the effects of using the helicopter as the maintenance vehicle on the reliability of OWF and the economy.

The use of ship for transportation has limitations. Weather conditions suitable for the maintenance are the wind speed $v(t) \leq 15$m/s, the significant wave height $h(t) \leq 2$m, and no lightning. As for the helicopter, it is not constrained by the significant wave height and the maximum wind speed for maintenance can be up to 17m/s [26]. Helicopters are relatively less affected by the severe weather than the ships.

The total yearly cost of using ships and helicopters are equal to their fixed rent plus the operating cost. Ships or helicopters are supposed to be used all year round. The estimated yearly cost of transportation tools are listed in Table 4. The electricity price is assumed to be 150 €/MWh [26]. Table 4 shows the results of *EENS* and the corresponding costs using ships or helicopters as transportation in case 5. It can be seen from Table 4 that the *EENS* cost after using helicopters is less than ships, which indicates that using helicopters can effectively improve the reliability of OWF.

TABLE 4. Reliability and economic comparison between cranes and helicopters.

	Transportation	*EENS* (MWh/y)	Cost of *EENS* (k€/y)	Yearly cost of vehicles (k€/y)	Total cost (k€/y)
Results	Ship	571492	85724	1800	87523
	Helicopter	550995	82649	9960	92609
Difference		20497	3075	-8160	-5085

TABLE 5. Annual weather characteristics in three different OWF locations.

Location	Average wind speed (m/s)	Maximum wind speed (m/s)	Average wave height (m)	Maximum wave height (m)
1	8.59	33.2	1.89	8.35
2	7.58	17.1	1.46	5.40
3	5.94	16.8	1.19	5.23

However, at the same time, the cost of using helicopters is significant high, leading to the rising total cost. Overall, it is uneconomical to use helicopters instead of ships in this scenario.

D. INFLUENCE OF WEATHER CHARACTERISTICS OF OWF LOCATION ON RELIABILITY

Reliability of the OWF depends on the weather conditions at the wind farm. Different OWF locations have different weather characteristics. This section examines the effects of wind speed and the significant wave height on the reliability of OWF. The weather characteristics at three locations are shown in Table 5. Fig. 8 shows the reliability evaluation results considering and without considering the effects of severe weather. It can be seen from Fig. 8 that *GRA* are basically the same without considering the severe weather effects, while *EENS* is different and inversely related to the average wind speed. This is mainly due to the fact that annual power generation of the wind farm decreases as the annual average wind speed decreases, resulting in an increase in *EENS* and a worse reliability level of OWF.

After considering severe weather, *GRA* is inversely related to the average wind speed and significant wave height of the sea area since it is difficult to reach OWF to perform maintenance when the wind speed and wave height are high, resulting in the deterioration of reliability of the failure component and eventually the decrease of *GRA*.

Compared to the situation where severe weather is not considered, the *EENS* for three areas considering severe weather conditions does not depend entirely on the annual average wind speed. For example, for the area 1 with a larger annual wind speed, *EENS* is larger than the area 2. Although the high wind speed will increase the power generation and reduce *EENS*, it will also influence the repair of the failure WT. This results in a reduction in the power generation

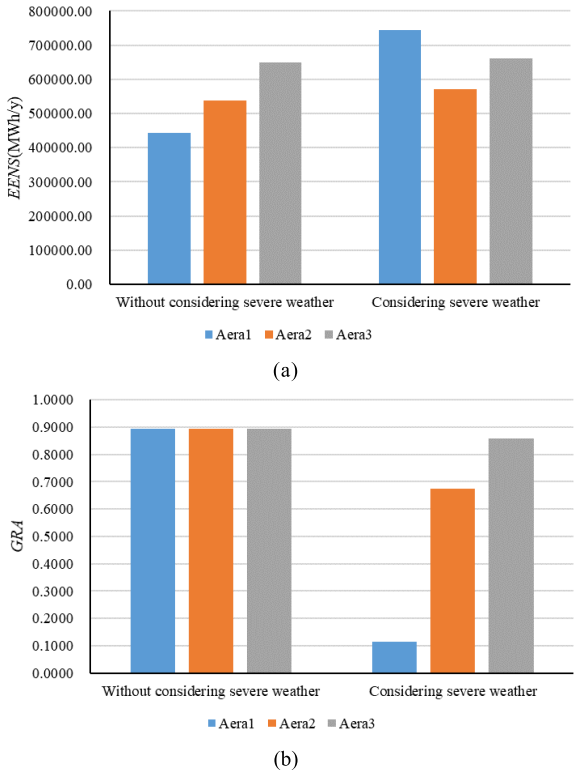

FIGURE 8. Reliability indices of different locations. (a) *EENS*. (b) *GRA*.

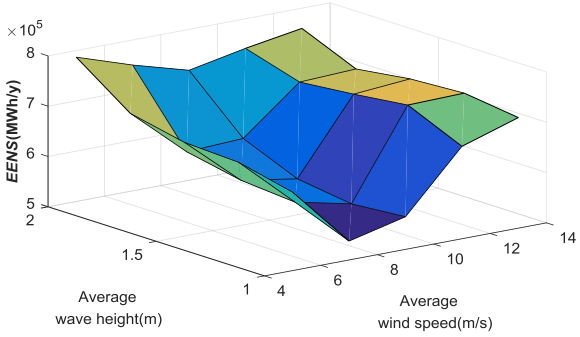

FIGURE 9. Reliability indices for different annual average wind speeds and annual average wave heights.

of the failure WT and ultimately leads to the deterioration of the reliability of the entire OWF.

Fig. 9 depicts the change of *EENS* under average annual wind speeds of 5m/s-13m/s and average annual wave heights of 1m-2m. This figure provides the influence of wind speed and wave height on the reliability of OWF. It can be seen from Fig. 9 that when the average significant wave height is constant, the *EENS* first decreases and then increases as the annual average wind speed increases, which is consistent with the conclusion drawn from Fig. 8. Keep the annual average wind speed constant, the waiting time and transportation time will increase as the significant wave height increases, resulting in an increase of *EENS* and lower reliability of OWF.

VI. CONCLUSION

The paper has presented a time-varying failure rate model of offshore WT and a time-varying repair time model of the OWF components considering the effects of severe weather. Reliability evaluation of OWF takes into account the correlation of the weather and component failure. In addition, a MCMC model is developed to simultaneously simulate the weather intensity and component state. The following conclusions are drawn from the case studies:

(1) Reliability indices *EENS* and *GRA* for OWF change significantly when the impact of severe weather on the WT failure rate and components repair time is considered.

(2) The impact of severe weather on the OWF reliability is mainly reflected on the repair process of components. Helicopters can increase the reliability of the OWF, but its cost of use is very high.

(3) The reliability of OWF depends not only on the wind sources in the sea area, but also on the weather conditions, such as significant wave height.

It is believed that the proposed model will improve the accuracy of the OWF reliability evaluation results and provide some useful guidelines for operator. For the future work, except for the influence of strong winds, lightning, and waves considered in this paper, the proposed model can be extended to integrate other types of severe weather. In addition, the reliability evaluation model can be incorporated in the planning stage of OWF to optimize its configuration in a more reliable manner.

REFERENCES

[1] EWEA. (2015). *Wind Energy Scenarios for 2030*. [Online]. Available: https://windeurope.org/fileadmin/files/library/publications/reports/EWEA-Wind-energy-scenarios-2030.pdf

[2] GWEC. (2017). *Global Wind Report Annual Market Update*. [Online]. Available: http://files.gwec.net/files/GWR2017.pdf?type= download

[3] R. Billinton and G. Bai, "Generating capacity adequacy associated with wind energy," *IEEE Trans. Energy Convers.*, vol. 19, no. 3, pp. 641–646, Sep. 2004.

[4] R. Billinton, H. Chen, and R. Ghajar, "A sequential simulation technique for adequacy evaluation of generating systems including wind energy," *IEEE Trans. Energy Convers.*, vol. 11, no. 4, pp. 728–734, Dec. 1996.

[5] P. Giorsetto and K. F. Utsurogi, "Development of a new procedure for reliability modeling of wind turbine generators," *IEEE Trans. Power App. Syst.*, vol. PAS-102, no. 1, pp. 134–143, Jan. 1983.

[6] X. Wang, H.-Z. Dai, and R. J. Thomas, "Reliability modeling of large wind farms and associateed electric utility interface systems," *IEEE Trans. Power App. Syst.*, vol. PAS-103, no. 3, pp. 569–575, Mar. 1984.

[7] C. Singh and A. Lago-Gonzalez, "Reliability modeling of generation systems including unconventional energy sources," *IEEE Trans. Power App. Syst.*, vol. PAS-104, no. 5, pp. 1049–1056, May 1985.

[8] R. A. Gonzalez-Fernandez and A. M. L. da Silva, "Reliability assessment of time-dependent systems via sequential cross-entropy Monte Carlo simulation," *IEEE Trans. Power Syst.*, vol. 26, no. 4, pp. 2381–2389, Nov. 2011.

[9] R. Billinton and R. Karki, "Application of monte carlo simulation to generating system well-being analysis," *IEEE Trans. Power Syst.*, vol. 14, no. 3, pp. 1172–1177, Aug. 1999.

[10] A. Sannino, H. Breder, and E. K. Nielsen, "Reliability of collection grids for large offshore wind parks," in *Proc. Int. Conf. Probabilities Meth. Appl. Power Syst. (PMAPS)*, Stockholm, Sweden, Jun. 2006, pp. 1–6.

[11] N. B. Negra, O. Holmstrom, B. Bak-Jensen, and P. Sorensen, "Aspects of relevance in offshore wind farm reliability assessment," *IEEE Trans. Energy Convers.*, vol. 22, no. 1, pp. 159–166, Mar. 2007.

[12] F. Katie. *This is Where the First U.S. Offshore Wind Turbines Were Just Installed*. Accessed: Jul. 2018. [Online]. Available: http://fortune.com/2016/08/08/first-us-offshore-wind/
[13] M. Scheu, D. Matha, M. Hofmann, and M. Muskulus, "Maintenance strategies for large offshore wind farms," *Energy Procedia*, vol. 24, pp. 281–288, Jan. 2012.
[14] I. Athamna, M. Zdrallek, E. Wiebe, and F. Koch, "Sensitivity analysis of offshore wind farm topology based on reliability calculation," in *Proc. Int. Conf. Probabilistic Methods Appl. Power Syst. (PMAPS)* Durham, U.K., Jul. 2014, pp. 1–6.
[15] Z. Lu, L. Cheng, and Y. Qiao, "Offshore wind power system reliability evaluation considering wind resource constraints and double weather patterns," (in Chinese), *Power Syst. Tech.*, vol. 39, no. 12, pp. 3536–3542, Dec. 2015.
[16] L.-L. Huang, Y. Fu, Y. Mi, J.-L. Cao, and P. Wang, "A Markov-chain-based availability model of offshore wind turbine considering accessibility problems," *IEEE Trans. Sustain. Energy*, vol. 8, no. 4, pp. 1592–1600, Oct. 2017.
[17] T.-Y. Lin and Y. Quéméner, "Extreme typhoon loads effect on the structural response of offshore meteorological mast and wind turbine," in *Proc. ASME 35th Int. Conf. Ocean, Offshore Arctic Eng.*, vol. 6, 2016, pp. 1–9.
[18] J.-S. Chou and W.-T. Tu, "Failure analysis and risk management of a collapsed large wind turbine tower," *Eng. Failure Anal.*, vol. 18, no. 1, pp. 295–313, Jan. 2011.
[19] J. Ribrant and L. M. Bertling, "Survey of failures in wind power systems with focus on swedish wind power plants during 1997–2005," *IEEE Trans. Energy Convers.*, vol. 22, no. 1, pp. 167–173, Mar. 2007.
[20] K. Alvehag and L. Soder, "A reliability model for distribution systems incorporating seasonal variations in severe weather," *IEEE Trans. Power Del.*, vol. 26, no. 2, pp. 910–919, Apr. 2011.
[21] S. Li, "Reliability models for DFIGs considering topology change under different control strategies and components data change under adverse operation environments," *Renew. Energy*, vol. 57, pp. 144–150, Sep. 2013.
[22] W. Li, *Risk Assessment of Power Systems: Models, Methods, and Applications*, 2nd ed. Piscataway, NJ, USA: Wiley, 2014.
[23] H.-X. Zhao and X.-R. Wang, "Lightning stroke mechanism of wind turbine generators and its lightning protection measures," (in Chinese), *Power Syst. Tech.*, vol. 27, no. 7, pp. 12–15, Jul. 2003.
[24] Y. Ji, K. Wu, L. Yin, J. Wang, and W. Zhou, "Analysis and protection of lightning damages for wind turbines," (in Chinese), *Shandong Electr. Power*, vol. 41, no. 5, pp. 20–30, May 2014.
[25] A. J. Eriksson, "The incidence of lightning strikes to power lines," *IEEE Power Eng. Rev.*, vol. PER-7, no. 7, pp. 66–67, Jul. 1987.
[26] F. Besnard, K. Fischer, and L. B. Tjernberg, "A model for the optimization of the maintenance support organization for offshore wind farms," *IEEE Trans. Sustain. Energy*, vol. 4, no. 2, pp. 443–450, Apr. 2013.
[27] P. Wang and R. Billinton, "Reliability cost/worth assessment of distribution systems incorporating time-varying weather conditions and restoration resources," *IEEE Trans. Power Del.*, vol. 17, no. 1, pp. 260–265, Jan. 2002.
[28] F. Cadini, G. L. Agliardi, and E. Zio, "A modeling and simulation framework for the reliability/availability assessment of a power transmission grid subject to cascading failures under extreme weather conditions," *Appl. Energy*, vol. 185, pp. 267–279, Jan. 2017.
[29] J. C. Spall, "Estimation via Markov chain Monte Carlo," *IEEE Control Syst.*, vol. 23, no. 2, pp. 34–45, Apr. 2003.
[30] A. Likas, N. Vlassis, and J. J. Verbeek, "The global k-means clustering algorithm," *Pattern Recognit.*, vol. 36, no. 2, pp. 451–461, Feb. 2003.
[31] Y. Guo, H. Gao, and Q. Wu, "A meteorological information mining-based wind speed model for adequacy assessment of power systems with wind power," *Int. J. Elect. Power Energy Syst.*, vol. 93, pp. 406–413, Dec. 2017.
[32] D. Li, W. Yan, W. Li, and Z. Ren, "A two-tier wind power time series model considering day-to-day weather transition and intraday wind power fluctuations," *IEEE Trans. Power Syst.*, vol. 31, no. 6, pp. 4330–4339, Nov. 2016.
[33] O. Dahmani, S. Bourguet, M. MacHmoum, P. Guérin, P. Rhein, and L. Jossé, "Optimization of the connection topology of an offshore wind farm network," *IEEE Syst. J.*, vol. 9, no. 4, pp. 1519–1528, Dec. 2015.
[34] C. Godsil and G. F. Royle, *Algebraic Graph Theory*. New York, NY, USA: Springer, 2001.
[35] M. Zhao, Z. Chen, and F. Blaabjerg, "Generation ratio availability assessment of electrical systems for offshore wind farms," *IEEE Trans. Energy Convers.*, vol. 22, no. 3, pp. 755–763, Sep. 2007.
[36] L. Huang and Y. Fu, "Reliability evaluation of the offshore wind farm," in *Proc. Asia–Pacific Power Energy Eng. Conf.*, Mar. 2010, pp. 1–5.
[37] NOAA. *National Data Buoy Center*. Accessed: Dec. 2018. [Online]. Available: https://www.ndbc.noaa.gov/historical_data.shtml#dart/
[38] J.-S. Chou, C.-K. Chiu, I.-K. Huang, and K.-N. Chi, "Failure analysis of wind turbine blade under critical wind loads," *Eng. Failure Anal.*, vol. 27, pp. 99–118, Jan. 2013.
[39] V. Peesapati, I. Cotton, T. Sorensen, T. Krogh, and N. Kokkinos, "Lightning protection of wind turbines—A comparison of measured data with required protection levels," *IET Renew. Power Gener.*, vol. 5, no. 1, pp. 48–57, Jan. 2011.